

# EraserDiT: Fast Video Inpainting with Diffusion Transformer Model

Jie Liu  
Mango TV

jieliu543@gmail.com

Zheng Hui  
Mango TV

zheng\_hui@aliyun.com

## Abstract

Video object removal and inpainting are critical tasks in the fields of computer vision and multimedia processing, aimed at restoring missing or corrupted regions in video sequences. Traditional methods predominantly rely on flow-based propagation and spatio-temporal Transformers, but these approaches face limitations in effectively leveraging long-term temporal features and ensuring temporal consistency in the completion results, particularly when dealing with large masks. Consequently, performance on extensive masked areas remains suboptimal. To address these challenges, this paper introduces a novel video inpainting approach leveraging the Diffusion Transformer (DiT). DiT synergistically combines the advantages of diffusion models and transformer architectures to maintain long-term temporal consistency while ensuring high-quality inpainting results. We propose a Circular Position-Shift strategy to further enhance long-term temporal consistency during the inference stage. Additionally, the proposed method automatically detects objects within videos, interactively removes specified objects, and generates corresponding prompts. In terms of processing speed, it takes only 180 seconds (testing on one NVIDIA A100 GPU) to complete a video with a resolution of  $1080 \times 1920$  with 121 frames without any acceleration method. Experimental results indicate that the proposed method demonstrates superior performance in content fidelity, texture restoration, and temporal consistency. Project page: [https://jieliu95.github.io/EraserDiT\\_demo/](https://jieliu95.github.io/EraserDiT_demo/).

## 1. Introduction

Video inpainting (VI) aims to synthesize appropriate content that is visually realistic, semantically accurate, and temporally consistent. This technique allows content creators to remove unwanted objects from original videos. Previously, mainstream VI methods have included flow-guided propagation and video Transformer.

The flow-guided propagation series [16] typically includes flow completion, feature propagation, and content

generation. The precision of flow completion directly impacts the quality of the final result. *ProPainter* [16] adopts a recurrent flow completion to provide precise optical flow fields for subsequent propagation modules. Equipped with dual-domain propagation and mask-guided sparse Transformer, *ProPainter* effectively performs propagation at the feature level between adjacent frames. However, when encountering large areas of masking, the generative capability of Generative Adversarial Networks (GANs) has been proven to be insufficient. As shown in Figure 1 and 2, this usually manifests as regular texture artifacts and blurrines.

Recently, diffusion models have gained popularity among researchers due to their superior performance in image and video generation. Li et al. [6] explored a video completion scheme based on the diffusion model (Animatediff [3]), attempting to address situations that previous methods struggled with (such as completing large gaps). They incorporate prior knowledge (inpainted by *ProPainter*) into the diffusion model to perform noise initialization. However, limited by the video generation capabilities of Animatediff, its ability to complete videos in fast-motion scenes is restricted.

Recently, text-to-video tasks based on diffusion transformer (DiT) models [4, 5, 13] have demonstrated highly commendable generation results. Unlike previous methods that use separated spatial and temporal attention to reduce computational complexity, these methods employ a 3D full attention mechanism to maintain the consistency of large-movement objects. These methods adopt 3D Variational Autoencoders (3D VAE) to implement video compression. Compared to the 2D VAE used by Animatediff, it not only compresses along the temporal dimension but also reduces the flickering issues in generated videos.

Consequently, leveraging the powerful generative capabilities and spatial-temporal consistency of video DiT, exploring large-gap and large-motion video inpainting is a feasible direction.

In this study, we developed an interactive video completion method based on video DiT architecture to handle large object removal tasks in high-resolution (up to 1080p) and large-motion scenes. Leveraging the powerful generative

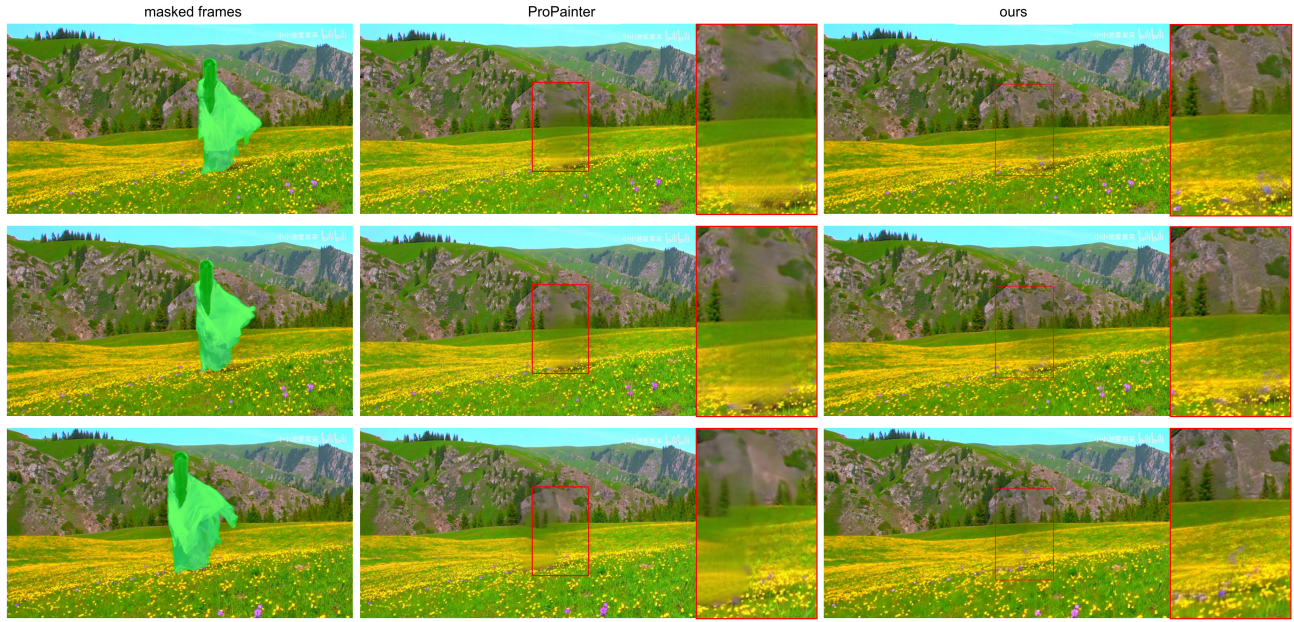


Figure 1. The results of video inpainting compared with *ProPainter*. In this figure, from the first column to the last column, the images display the masked video frames, *ProPainter*’s completion results, and the proposed method’s completion results, respectively. Notably, when examining the completion area in greater detail, it becomes apparent that *ProPainter*’s method exhibits more severe artifacts and lacks the enhanced textures and details, but the proposed method provides.



Figure 2. This example involves removing the little girl from the video. From left to right, the images represent the masked video, *ProPainter*’s results, and our results. As shown, *ProPainter*’s completion results lack ribbon consistency in the temporal domain. Additionally, the leaves are devoid of texture and the overall output fails to exhibit spatial domain consistency.

capabilities of the foundational text-to-video large model, we can remove various types of objects, including people, animals, plants, vehicles, subtitles, and other common targets. The main contributions of this work can be summarized as follows.

- This paper introduces DiT for maintaining spatiotemporal consistency in high-resolution videos during object removal tasks. DiT employs 3D full attention to enhance spatiotemporal consistency and leverages the high downsampling scale of the 3D Causal VAE to efficiently process high-resolution video object removal up to 1080p.
- To better maintain temporal consistency, we propose an inference method called the Circular Position-Shift strategy.
- To facilitate the removal of large objects in high-resolution videos (up to 1080p) with significant motion, this work generated approximately 60,000 mask videos for dynamic objects, including people and animals.
- To improve usability and achieve more accurate video descriptions during the testing phase, we propose an automated method for generating text prompts for videos that do not contain the object to be removed. This approach guarantees a more efficient and precise alignment between the video content and the descriptive text.

## 2. Related Work

### 2.1. Video Inpainting

The current mainstream video inpainting methods can be broadly categorized into Flow-Guided Propagation-based and Video Transformer-based approaches. Flow-guided propagation has become a pivotal technique in video inpainting, leveraging completed optical flow to align frames seamlessly while ensuring temporal coherence throughout the video.

Turning attention to Video Transformers, a groundbreaking approach in this field is STTN [15], which incorporates ViT [1] into video inpainting, providing an effective solution to address both spatial and temporal dimensions simultaneously. Liu et al. [8] advanced this approach by refining transformer-based methods, improving the sub-token fusion ability of transformers for learning fine-grained features to better replicate the dynamics in video sequences.

Among these methods, Propainter [16] emerges as a notable approach, featuring recurrent flow completion, dual-domain propagation, and a mask-guided sparse Transformer. This method excels at propagating known pixels across all frames and showcases an early capability to synthesize unknown pixels. However, its generative capacity faces limitations when handling large masks, often resulting in visible artifacts.

### 2.2. Video Generation with DiT

By leveraging Transformers as the foundation for diffusion models, specifically Diffusion Transformers (DiT), text-to-video generation has achieved a remarkable new milestone. Early notable work in the open-source community includes CogVideoX [13], which introduces 3D full attention to replace the separated spatial and temporal attention, effectively resolving inconsistency issues in the generated videos. CogVideoX primarily utilizes the multi-modal DiT (MM-DiT) architecture [2] and incorporates the Expert Adaptive LayerNorm to independently handle each modality. HunyuanVideo [5] integrates a combination of multi-stream DiT and single-stream DiT architectures, successfully training a video generation model with over 13 billion parameters. This model surpasses the performance of previous state-of-the-art models, such as Runway Gen 3 and Luma 1.6. HunyuanVideo’s exceptional generative performance is commendable. However, it requires significantly more GPU memory consumption (60GB needed for 129 frames at 720p resolution) and has slower inference speeds. Recently, the Lightricks Team proposed LTX-Video [4], a real-time video latent diffusion method. Its greatest advantage is its inference speed, thanks to the design of a 1 : 192 compression ratio with spatiotemporal downsampling of  $32 \times 32 \times 8$ , enabling the generation of high-resolution video at unprecedented speed. Although LTX-Video’s performance is not as good as HunyuanVideo, it offers a better balance between performance and speed, and the strong reference nature of video completion tasks means that the generative capability requirement is lower compared to pure text-to-video tasks. Therefore, we chose LTX-Video as our backbone model.

## 3. Methodology

There are severe artifacts and unnatural textures in the flow-guided method. Therefore, this paper proposes a new method. We present a novel algorithm leveraging the diffusion transformer (DiT) with simple prompts to significantly enhance video object removal tasks. This approach adeptly addresses three key challenges: enabling the direct removal and completion of objects in 1080p resolution videos to maintain high-quality and detailed results; automatically detecting objects within videos and interactively removing specified objects with automated prompt generation; and effectively completing large masked regions, ensuring the superior removal of humans and other common targets. By combining the strengths of diffusion models and transformer architectures, our method not only improves long-term temporal consistency and quality inpainting but also establishes a robust and efficient solution for complex video inpainting challenges, advancing the state-of-the-art in video object removal and completion tasks. The specific

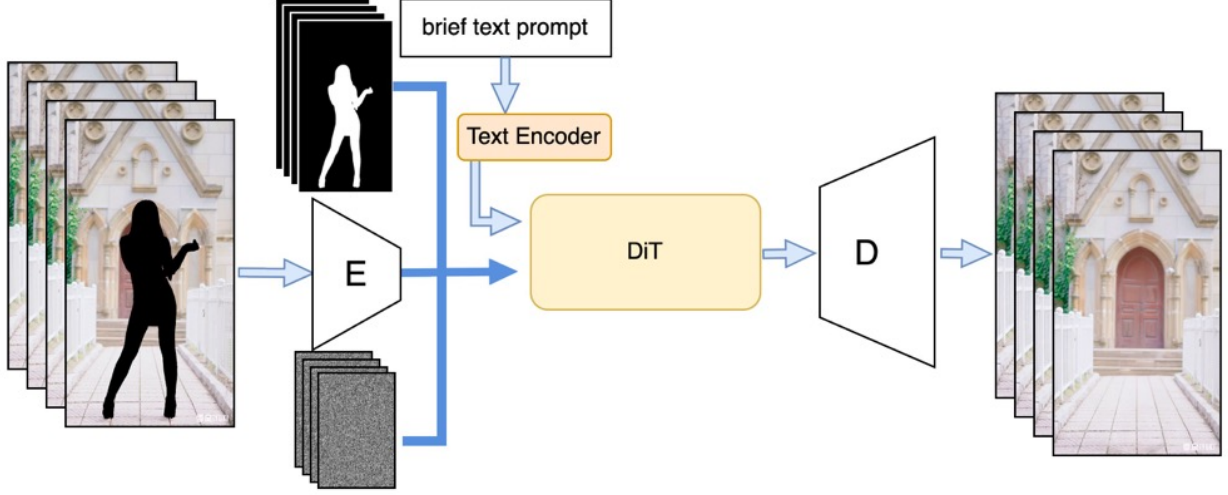


Figure 3. The training pipeline of the proposed method for video object removal. In this method, the pipeline requires three inputs: a masked video sequence, a mask video, and a corresponding brief text prompt. The masked video sequence undergoes encoding by the VAE to obtain latent features. These features are then concatenated with the noise and the downsampled mask sequence in the spatiotemporal domain along the channel dimension. During the training phase, fine-tune all the parameters of the video transformer while keeping the other parameters frozen.

methods are comprehensively detailed in the following subsections.

### 3.1. Training pipeline

In the task of video object removal, both speed and quality are crucial. To address this, we have chosen *LTX-Video* [4] as our foundational architecture. As illustrated in Figure 3, this architecture integrates a VAE, a text encoder, and a denoising video transformer, whose inputs are masked video sequence, the corresponding mask sequence, and the corresponding text prompt. During the training stage, we randomly select a video  $V_i$  from various videos  $V = \{V_1, V_2, V_3, \dots, V_n\}$  and a mask video  $M_j$  from various masks  $M = \{M_1, M_2, M_3, \dots, V_n\}$ . These videos are then inputted into the model for training.

The latent features are extracted from the masked video sequence  $V_M = V_i * M_j$  using the 3D VAE encoder, which performs spatiotemporal downsampling at a scale of  $32 \times 32 \times 8$ . Following this, the corresponding mask sequence is downsampled to the same scale, ensuring consistency. However, given that the 3D VAE encoder of *LTX-Video* employs 3D Causal Convolutions, the temporal features consist of  $1 + \frac{n-1}{8}$  frames. Consequently, in the temporal domain, the masks  $M_j^{input}$  of eight temporally contiguous mask frames  $M_j$  are intersected to form a single mask frame, except for the first frame mask. Ultimately, the input to the denoising video transformer combines the latent features of the masked video sequence with the spatiotemporally downsampled mask sequence, as shown in Figure

3.

Furthermore, since the video containing the object to be removed is confined to a single scene, a brief prompt specific to that scene suffices. During the training stage, the pre-obtained prompt is encoded by the text encoder [10] to generate the prompt embeddings, which serve as an additional input for the denoising video transformer. Feature fusion between the prompt embedding tokens and the masked video feature tokens is achieved through cross-attention.

### 3.2. Inference pipeline

During the testing stage, to enhance usability and achieve more precise video descriptions, we propose implementing an automated prompt method to generate text prompts. This approach ensures a more efficient and accurate alignment between the video content and the descriptive text. Therefore, we adopt the VLM method for video understanding and obtain its prompt.

The complete inference pipeline is illustrated in Figure 4. Initially, we employ *MiniCPM-o*<sup>1</sup> [14] to detect objects present in the video  $V_{test}$  and generate a scene description. Subsequently, the user selects the name of the object to be removed. Through an iterative dialogue process, we then produce a video description that excludes the specified object. In addition, based on the prompt provided by the user for the object to be removed, a mask sequence  $M_{test}$  can be obtained. Therefore, the masked video sequence  $V_{test}^{masked}$  is obtained by applying a pixel-wise multiplica-

<sup>1</sup><https://github.com/OpenBMB/MiniCPM-o>

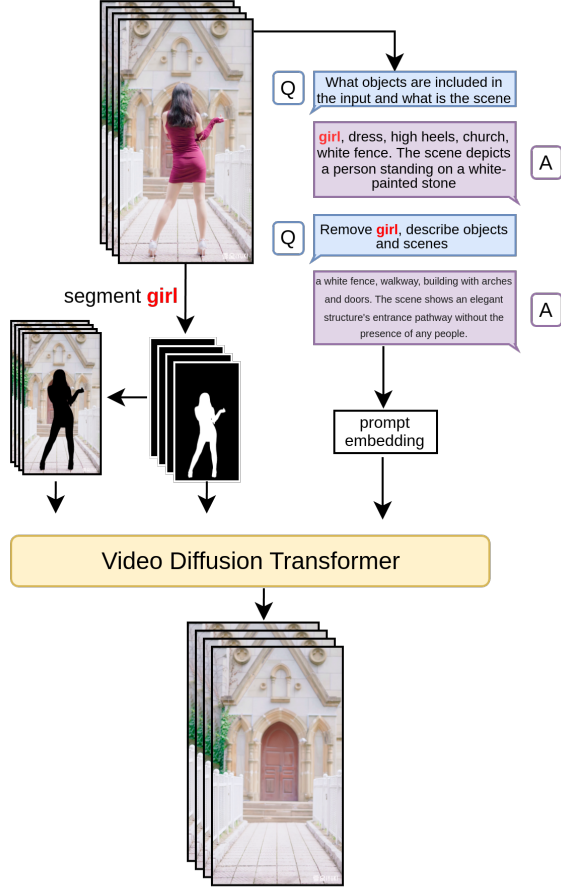


Figure 4. The inference pipeline of the proposed method for video object removal. As illustrated in the figure, in multiple rounds of dialogue with the VLM, “Q” and “A” represent fixed question formats and VLM’s answers, respectively, used for interacting with the user and generating automated prompts that exclude the object to be removed.

tion of the video  $V_{test}$  and the mask sequence  $M_{test}$ , that is  $V_{test}^{masked} = V_{test} * M_{test}$ . At this stage, we have gathered all the necessary input conditions. By feeding these inputs into the model, we perform inference to obtain the final completed video  $V_{out}$  without the target object.

To maintain consistency in the temporal domain, this paper proposes the Circular Position-Shift strategy for long sequences (as described in Figure 5 and Algorithm 1) that exceed the maximum training sequence length. In detail, we first pad the input sequence using the reflect mode. Next, we concatenate the beginning and the end to form a circular sequence. In a circular sequence, any selected subsequence is a physically coherent video segment. We set a cumulative shift offset, denoted as  $\alpha_\sigma$ , accumulating  $\alpha$  at each timestep. This ensures that the model initiates the sliding window from different positions. Although using this strat-

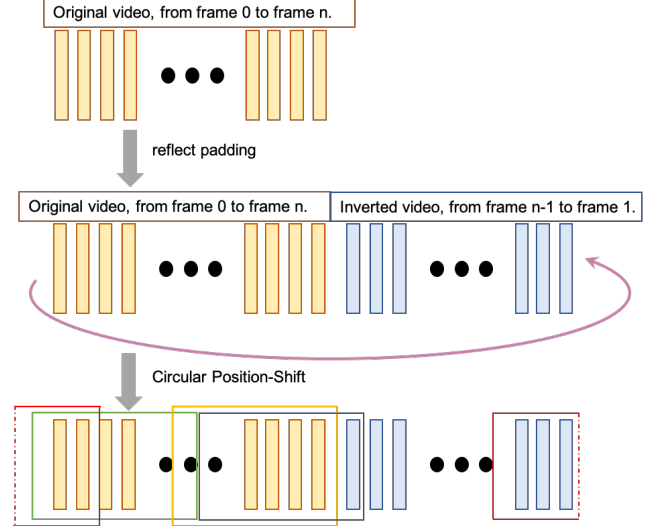


Figure 5. The Circular Position-Shift strategy involves reflect padding the original video sequence, which spans from frame 0 to frame  $n$ . After padding, the sequence extends from frame  $(n-1)$  to frame 1, and the two sequences are concatenated. Circular Position-Shift is then applied for inference.

#### Algorithm 1 Circular Position-Shift for Long Sequence

**Require:** Masked video embedding  $c_{mv}^{[0,l]}$  and mask map  $c_m^{[0,l]}$  with length  $l$ , denoising steps  $T$ , initial noisy latent  $z_T^{[0,T]}$ , pretrained EraserDiT model  $ED(\cdot)$  for sequence length  $f$ , position-shift offset  $\alpha$ .

**Ensure:** Denoised latent  $z_0^{[0,l]}$ .

- 1: Initialize accumulated shift offset  $\alpha_\sigma = 0$
- 2: // Reflect sequence to construct circular sequence
- 3:  $c_{mv}^{[0,l]+[l-1,1]}$ ,  $c_m^{[0,l]+[l-1,1]}$ , circular sequence length  $L = 2l - 2$ .
- 4:  $indices = [0, l] + [l - 1, 1]$
- 5: **for**  $t = T$  **to** 1 **do**
- 6:   // Denoising loop
- 7:   Initialize start point  $s = \alpha_\sigma$ , end point  $e = s + f$ , processed length  $pl = 0$ .
- 8:   // pad mode is warp
- 9:    $curr\_indices = right\_pad(indices, \alpha_\sigma)$
- 10:   **while**  $pl < L$  **do**
- 11:      $curr\_idx = curr\_indices[[s, e]]$
- 12:      $z_{t-1}^{curr\_idx} = ED(z_t^{curr\_idx}, c_{mv}^{curr\_idx}, c_m^{curr\_idx}, t)$   
 $s \leftarrow s + f, e \leftarrow e + f, pl \leftarrow pl + f$ .
- 13:   **end while**
- 14:    $\alpha_\sigma \leftarrow \alpha_\sigma + \alpha$
- 15: **end for**
- 16: **return** Denoised latent  $z_0^{[0,l]}$ .

egy results in nearly double the inference cost, we employ the classifier-free guidance (CFG) distillation model to re-

duce the inference cost back to its original level. We distill the combined outputs of unconditional and conditional inputs into a single student model. Specifically, the student model is conditioned on a guidance scale and shares the same structures and hyperparameters as the teacher model. We initialize the student model with the same parameters as the teacher model and train it using a fixed guidance scale 3.0.

## 4. Experiments

### 4.1. Training Data

In the task of video object removal, obtaining paired training data (videos containing the target and corresponding ground truth without the target) is very challenging and unnecessary. Therefore, we will utilize synthetic data for training. This synthetic data encompasses a diverse range of background videos  $V = \{V_1, V_2, V_3, \dots, V_n\}$  and various masks  $M = \{M_1, M_2, M_3, \dots, M_n\}$ . To achieve this, we downloaded 600,000 diverse background videos from the *Pexels* website<sup>2</sup>. These videos encompass a variety of types, including landscapes, grasslands, buildings, mountains, and rivers. The mask data is composed of three components: masks from the open-source SA-V dataset [11], animal masks, and human masks. The latter two were obtained by crawling the internet for videos of animals moving and people dancing videos, whose masks are extracted by SAM 2 [11].

**Animal masks.** We first downloaded video clips of large animals from the material video website. Since these videos generally lack scene changes, we extracted the masks according to their categories. Ultimately, we obtained approximately 30,000 videos, each with a duration ranging from 1 to 5 seconds.

**Human masks.** Firstly, we need to download the raw videos containing people from the Internet, due to the characters lacking diversity in the material video website. To achieve more accurate tracking of the specified person and obtain their mask in the video, we exclusively retain single-person video clips through Object Detection. To ensure the continuity of target movement, it is crucial to avoid scene transitions within video clips. Initially, we utilized PySceneDetect for preliminary scene segmentation due to its speed, despite its lower accuracy. After that, for a more precise extraction of video clips without scene transitions or target switches, we employ manual annotation to obtain the final video clips. Finally, we tracked the human and extracted its masks from all video clips using Grounded SAM 2 [12] and saved them. We processed approximately 32,000 videos, each with a duration ranging from 5 to 20 seconds.

<sup>2</sup><https://www.pexels.com>

## 4.2. Training Details

We utilize *LTX-Video* [4] as the foundational architecture. We only train the parameters of the video transformer model for video inpainting, whose training details are described in Section 4.2.1. However, we found the presence of severe artifacts after the 3D VAE of *LTX-Video* [4], so we finetune the parameters of the VAE Decoder and freeze the Encoder’s, whose fine-tune details are described in Section 4.2.2.

### 4.2.1. Video Transformer

The video transformer is trained with a resolution of  $960 \times 960$  and 81 frames. The training process comprises 280k iterations on 24 NVIDIA A100 (80G) GPUs, utilizing the *Adam-W* optimizer with an initial learning rate of  $3 \times 10^{-5}$ . In addition, to achieve faster and more stable training, the *Rectified Flow* [7] is employed. The loss function is implemented in two distinct stages. In the first stage, spanning the initial 150k iterations, we exclusively utilize the L2 loss function to optimize the video transformer. To enhance the handling of video object removal with significant motion, the frame sampling step is randomly chosen from 1 to 6 during the training phase.

Subsequently, in the second stage, we shift our focus to the masked region by employing the Focal Area loss function for the remaining iterations. Focal Area loss is defined by

$$L_{focal} = L_2 * (1 + D_{mask}), \quad (1)$$

and the  $D_{mask}$  is the dilated mask pf  $M_j^{input}$ .

### 4.2.2. VAE Decoder

As illustrated in Figure 6, the original VAE of *LTX-Video* exhibits chessboard artifacts in scenarios involving significant motion, particularly evident in the final frame. Therefore, we fine-tuned the decoder section of the VAE. In addition to the commonly used  $L_1$  reconstruction loss, we integrate perceptual loss  $L_{dists}$  and GAN adversarial loss  $L_{adv}$  to further improve the quality of reconstruction. The complete loss function is shown in Equation 2.

$$Loss_{vae} = L_1 + L_{dists} + 0.05L_{adv} \quad (2)$$

## 4.3. Performance Evaluation

**Spatial results.** The comparative results are presented in Figure 8. While *ProPainter* exhibits more artifacts and inaccuracies in its completions, our method demonstrates fewer artifacts and accurately reproduces the natural textures of water waves and trees. Consequently, our method is capable of generating more detailed and textured outputs.

**Temporal results.** In the temporal domain, our results maintain good consistency throughout the entire video sequence compared to *ProPainter*, as shown in Figure 9. The bridge completed by *ProPainter* is not straight and exhibits

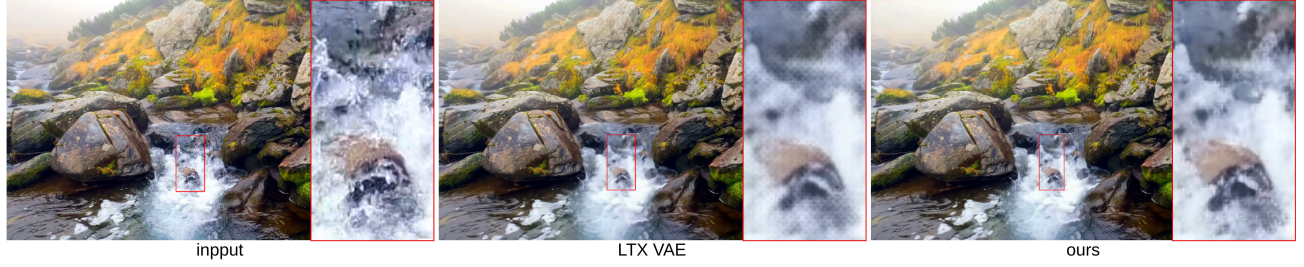


Figure 6. The results of VAE compared with *LTX-Videp*. In this figure, from the first column to the last column, the images display the input, the result of *LTX-Videp* VAE, and our finetuned VAE, respectively.

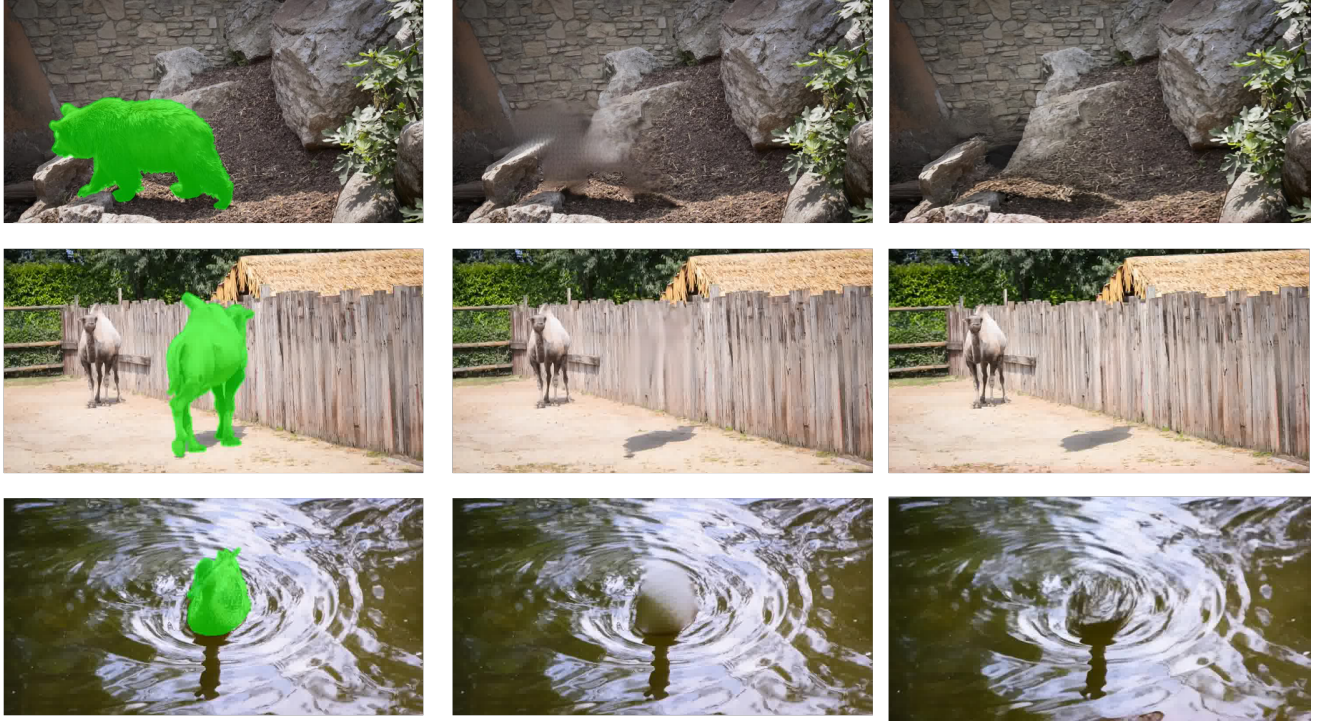


Figure 7. The results on the DAVIS dataset are presented as follows: the first column shows the input masked frames, the second column displays the results of ProPainter, and the third column contains our results.

ghosting, as indicated by the red box in the second row of Figure 9. In contrast, our method produces a consistent bridge in each frame, as seen in the last row of Figure 9.

**Evaluation on DAVIS.** The visual results on DAVIS dataset [9] are shown in Figure 7. Upon observation, it becomes evident that our method excels in reconstructing textures consistent with the background during the removal of large objects, while ProPainter’s completed areas are marred by numerous unnatural artifacts. Moreover, in regions characterized by patterns such as stripes or water ripples, ProPainter struggles to accurately capture their natural states. In contrast, our method effectively represents these natural patterns and the dynamics of water movement.

Besides, we generate masks and then reconstruct masked

videos by EraserDiT on DAVIS dataset [9], allowing for the calculation of quantitative scores. As is widely known, video completion tasks focus more on visual quality. Therefore, we employ LPIPS, SSIM, and FVD as quantitative evaluation metrics to comprehensively assess the visual consistency and perceptual quality of the generated videos. Table 1 shows that the proposed method outperforms ProPainter across all quantitative metrics.

Finally, regarding the inference time, the proposed method takes only 180 seconds to complete for a video with a resolution of  $1080 \times 1920$  and 121 frames with 40 step denoising on a single A100 GPU. Thus, the proposed method delivers swift inference while maintaining superior visual quality, striking an optimal balance between speed and per-

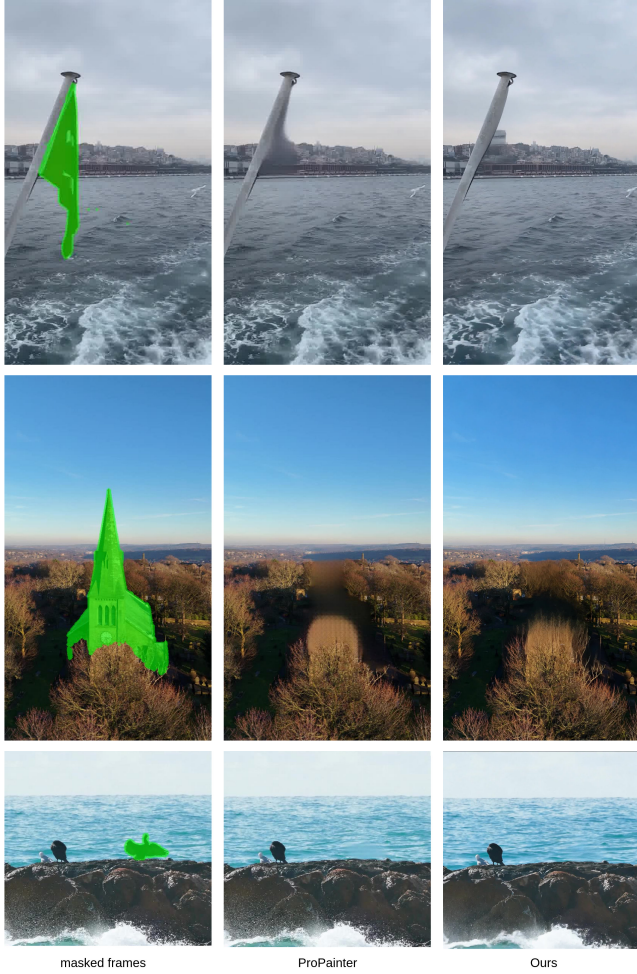


Figure 8. The results of ProPainter and the proposed method. There are more textures and fewer artifacts in the proposed method.

Table 1. Quantitative comparisons on DAVIS datasets

Method	SSIM $\uparrow$	LPIPS $\downarrow$	FVD $\downarrow$
ProPainter	0.9492	0.0379	120.53
Ours(EraserDiT)	<b>0.9673</b>	<b>0.0320</b>	<b>87.08</b>

formance. The results of target removal and completion in other videos will be presented in the supplementary material.

## 5. Limitations

Due to the inherent limitations of the current video generation fundamental mode, the results are suboptimal in scenarios involving rapidly flowing water and extremely fast

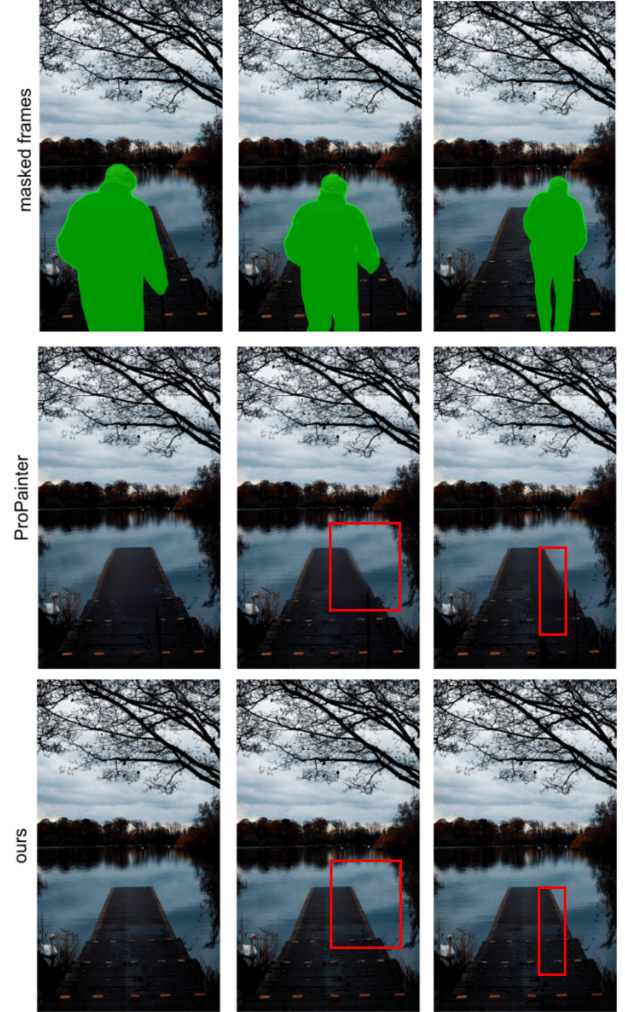


Figure 9. The results of ProPainter and the proposed method. They demonstrate the context consistency in the temporal domain.

camera movements. In future work, our aim is to address these challenges by incorporating alternative fundamental modes of video generation to improve performance in such complex scenes.

## 6. Conclusion

In this paper, we present a novel video object removal method based on the DiT model. Additionally, we propose a data processing workflow for obtaining large object masks, along with an automated method for generating text prompts for videos that do not contain the object to be removed. This approach effectively removes large objects in high-resolution videos, even in the presence of significant motion. The visual quality of the completed areas after object removal demonstrates state-of-the-art performance in

terms of both texture and detail.

## References

- [1] Alexey Dosovitskiy, Lucas Beyer, Alexander Kolesnikov, Dirk Weissenborn, Xiaohua Zhai, Thomas Unterthiner, Mostafa Dehghani, Matthias Minderer, Georg Heigold, Sylvain Gelly, et al. An image is worth 16x16 words: Transformers for image recognition at scale. *arXiv preprint arXiv:2010.11929*, 2020. 3
- [2] Patrick Esser, Sumith Kulal, Andreas Blattmann, Rahim Entezari, Jonas Müller, Harry Saini, Yam Levi, Dominik Lorenz, Axel Sauer, Frederic Boesel, et al. Scaling rectified flow transformers for high-resolution image synthesis. In *Forty-first international conference on machine learning*, 2024. 3
- [3] Yuwei Guo, Ceyuan Yang, Anyi Rao, Zhengyang Liang, Yaohui Wang, Yu Qiao, Maneesh Agrawala, Dahua Lin, and Bo Dai. Animatediff: Animate your personalized text-to-image diffusion models without specific tuning. *arXiv preprint arXiv:2307.04725*, 2023. 1
- [4] Yoav HaCohen, Nisan Chiprut, Benny Brazowski, Daniel Shalem, Dudu Moshe, Eitan Richardson, Eran Levin, Guy Shiran, Nir Zabari, Ori Gordon, et al. Ltx-video: Realtime video latent diffusion. *arXiv preprint arXiv:2501.00103*, 2024. 1, 3, 4, 6
- [5] Weijie Kong, Qi Tian, Zijian Zhang, Rox Min, Zuozhuo Dai, Jin Zhou, Jiangfeng Xiong, Xin Li, Bo Wu, Jianwei Zhang, et al. Hunyuanvideo: A systematic framework for large video generative models. *arXiv preprint arXiv:2412.03603*, 2024. 1, 3
- [6] Xiaowen Li, Haolan Xue, Peiran Ren, and Liefeng Bo. Diffuseraser: A diffusion model for video inpainting. *arXiv preprint arXiv:2501.10018*, 2025. 1
- [7] Yaron Lipman, Ricky TQ Chen, Heli Ben-Hamu, Maximilian Nickel, and Matt Le. Flow matching for generative modeling. *arXiv preprint arXiv:2210.02747*, 2022. 6
- [8] Rui Liu, Hanming Deng, Yangyi Huang, Xiaoyu Shi, Lewei Lu, Wenxiu Sun, Xiaogang Wang, Jifeng Dai, and Hongsheng Li. Fuseformer: Fusing fine-grained information in transformers for video inpainting. In *Proceedings of the IEEE/CVF international conference on computer vision*, pages 14040–14049, 2021. 3
- [9] Federico Perazzi, Jordi Pont-Tuset, Brian McWilliams, Luc Van Gool, Markus Gross, and Alexander Sorkine-Hornung. A benchmark dataset and evaluation methodology for video object segmentation. In *Proceedings of the IEEE conference on computer vision and pattern recognition*, pages 724–732, 2016. 7
- [10] Colin Raffel, Noam Shazeer, Adam Roberts, Katherine Lee, Sharan Narang, Michael Matena, Yanqi Zhou, Wei Li, and Peter J Liu. Exploring the limits of transfer learning with a unified text-to-text transformer. *Journal of machine learning research*, 21(140):1–67, 2020. 4
- [11] Nikhila Ravi, Valentin Gabeur, Yuan-Ting Hu, Ronghang Hu, Chaitanya Ryali, Tengyu Ma, Haitham Khedr, Roman Rädle, Chloe Rolland, Laura Gustafson, Eric Mintun, Junting Pan, Kalyan Vasudev Alwala, Nicolas Carion, Chao-Yuan Wu, Ross Girshick, Piotr Dollár, and Christoph Feichtenhofer. Sam 2: Segment anything in images and videos, 2024. 6
- [12] Tianhe Ren, Shilong Liu, Ailing Zeng, Jing Lin, Kunchang Li, He Cao, Jiayu Chen, Xinyu Huang, Yukang Chen, Feng Yan, et al. Grounded sam: Assembling open-world models for diverse visual tasks. *arXiv preprint arXiv:2401.14159*, 2024. 6
- [13] Zhuoyi Yang, Jiayan Teng, Wendi Zheng, Ming Ding, Shiyu Huang, Jiazheng Xu, Yuanming Yang, Wenyi Hong, Xiaohan Zhang, Guanyu Feng, et al. Cogvideox: Text-to-video diffusion models with an expert transformer. *arXiv preprint arXiv:2408.06072*, 2024. 1, 3
- [14] Yuan Yao, Tianyu Yu, Ao Zhang, Chongyi Wang, Junbo Cui, Hongji Zhu, Tianchi Cai, Haoyu Li, Weilin Zhao, Zhihui He, et al. Minicpm-v: A gpt-4v level mllm on your phone. *arXiv preprint arXiv:2408.01800*, 2024. 4
- [15] Yanhong Zeng, Jianlong Fu, and Hongyang Chao. Learning joint spatial-temporal transformations for video inpainting. In *Computer Vision—ECCV 2020: 16th European Conference, Glasgow, UK, August 23–28, 2020, Proceedings, Part XVI 16*, pages 528–543. Springer, 2020. 3
- [16] Shangchen Zhou, Chongyi Li, Kelvin CK Chan, and Chen Change Loy. Propainter: Improving propagation and transformer for video inpainting. In *Proceedings of the IEEE/CVF International Conference on Computer Vision*, pages 10477–10486, 2023. 1, 3